

# Cu<sub>1-x</sub>Sr<sub>x</sub>TiO<sub>3</sub> thin film resistors for Carbon Monoxide sensing

Rajendrakumar Banshilal Ahirrao\*<sup>1</sup> and Vijay Namdeo Pawar<sup>2</sup>

\*<sup>1</sup>Department of Physics, Uttamrao Patil Arts and Science College, Dahiwel, Dist.-Dhule-424302, Maharashtra (India)

\*<sup>2</sup>Department of Physics, Siddhartha College Fort Mumbai, Maharashtra, India

E-mail: [ahirraorb@gmail.com](mailto:ahirraorb@gmail.com) [vijaynpawar12345@gmail.com](mailto:vijaynpawar12345@gmail.com)

**Abstract:** Thin films of pure and CuO-modified SrTiO<sub>3</sub> (STO) were prepared by spray pyrolysis technique. The Cu<sub>1-x</sub>Sr<sub>x</sub>TiO<sub>3</sub>; Cu 0.1weight% thin films were prepared by spraying aqueous solution Sr (Cl<sub>2</sub>)6H<sub>2</sub>O, TiCl<sub>3</sub> and CuCl<sub>2</sub> precursors. Prepared films were fired at 500<sup>o</sup> C for 30 min. The Cu<sub>1-x</sub>Sr<sub>x</sub>TiO<sub>3</sub>(x=0.1 to 0.9) thin films were prepared by spray pyrolysis method. From XRD profiles, effect of Cu concentration on the crystal structure, average particle size and lattice parameter were investigated. The gas sensing properties of pure and CuO modified STO thin films were investigated for various gases on homemade static gas sensing system. The maximum gas response (2000) was obtained for CuO doped STO thin films. The CuO modification has significant effect on sensing performance. The instant response T<sub>25</sub> and fast recovery T<sub>45</sub> are main features of sensor. The structural properties of the films were estimated using X-ray diffraction study. The particle properties were analyzed by FE-SEM and EDS analysis. Selectivity, response and recovery times were investigated and discussed.

**Keywords:** STO, thin films, CuO doping, Carbon Monoxide, sensor.

## 1. Introduction

Environment pollution is monotonically increasing due to combustible and process gases mainly from industry and motor vehicles. To protect environment, it is essential to control and safely monitor the pollution. Different methods like gas chromatography, infrared spectroscopy, semiconductor gas sensors and many others have been used to detect and monitor the pollutants. But solid-state semiconducting gas sensors have considerable advantages than the other gas detection techniques. Semiconducting sensors are reliable, easy to miniaturize, less costly, easy to produce, and can be designed to operate over a wide range of conditions. It can also operate at high temperatures. Semiconducting sensors can be designed for sensing of multiple species simultaneously and also detection limits are in the range of part per million levels (ppm).

It is a fact that the sensor characteristics can be changed by varying the crystal structure, dopants, preparation method, operation temperature, etc. Nonetheless, highly specific metal-oxide sensors are still not available. In recent years, the interest of researchers and engineers to gas sensitive materials has grown substantially due to the progress in thin film technology. Many semiconducting metal oxides have been used as gas sensors. Many different semiconducting oxides in bulk ceramic, thick film, and thin film forms have been studied as a sensor element for gas sensing<sup>4,5</sup>. The perovskite oxides (ABO<sub>3</sub>) were used as gas sensor materials for their stability in ther-

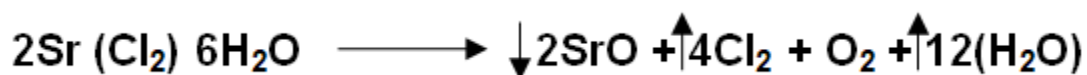
mal and chemical atmospheres. Modifications in microstructure, processing parameters and also concentration of acceptor/donor dopant can vary the temperature coefficient of the resistance and conductivity of  $ABO_3$  oxides. Sensors based on  $ABO_3$ -type complex oxide material, of rare earth elements have an outstanding merit of its highly sensitive and selective characteristics.

Development of gas sensors using un-doped/ doped metal oxides and  $ABO_3$  for the detection of gases like  $NO_2$  [1], CO [2-4]  $H_2$  [5-6]  $NH_3$  [7],  $H_2S$  [8-9] has already been reported. Carbon monoxide (CO) is a gas that is flammable, poisonous, colorless, and tasteless. Because of it is not colored and tasteless carbon monoxide is difficult to detect when without using detection technology [10]. Therefore, carbon monoxide is often dubbed the "silent killer", and needed a technology that can detect the presence of CO gas. The gas sensor for the detection of carbon monoxide gas which is contained in automobile exhaust along with nitrogen oxides is the most important environmental contaminant and represents a challenging job for researchers Lim et al., Qian et al., and Ramirez et al. have studied the detection of CO gas at a temperature of  $400^\circ C$ ,  $250^\circ C$ - $300^\circ C$  and  $295^\circ C$ , respectively, with sensing materials ZnO,  $SnO_2Au$  and  $SnO_2$ , respectively. But the present paper describes the detection of CO gas at low temperature of  $220^\circ C$  by synthesizing thin film of  $SnO_2$  on glass substrate by sol-gel method. Till today so many methods were adopted to synthesize doped or un-doped tin oxide films such as Thermal Evaporation [11-12], Chemical Vapor Deposition [13-14], R.F. Magnetron CO sputtering [15] Laser Pulse Evaporation [16-17], Spray Pyrolysis [18-19], ultrasonic spray pyrolysis [20], and sol-gel [21-23]. Among these techniques Spray Pyrolysis method is most useful method because of its easy operation and capability to make various conducting, semiconducting and gas sensing applications of thin films.

## 2. Material and Methods

### 2.1. Experimental

The pure STO and Cu modified STO thin films are prepared by spray pyrolysis technique. High-purity inorganic salts,  $CuCl_2$ ,  $Sr(Cl_3)6H_2O$  and  $TiCl_3$  were employed as the starting ingredients for pure and modified STO thin films. The stoichiometric amount of each salt with cation ratios of Sr:Ti=1:1 (0.1M) was dissolved in d-ionized water and solution is stir for 30min on magnetic stirrer. The formation of pure STO thin films was achieved according to the following chemical reaction.



The Cu modified semiconductor type  $CuO-SrTiO_3$ -based thin films were obtained by doping copper. The stoichiometric amount of each salt with cation ratios of Cu:Sr: Ti=1:1:1 (Cu 0.1M) was dissolved in d-ionized water and solution is stir for 30min on magnetic stirrer. The resultant solution was sprayed on glass substrate kept at  $350 \pm 50^\circ C$ . When the solution is sprayed, the reaction takes place at the surface of the preheated substrate.

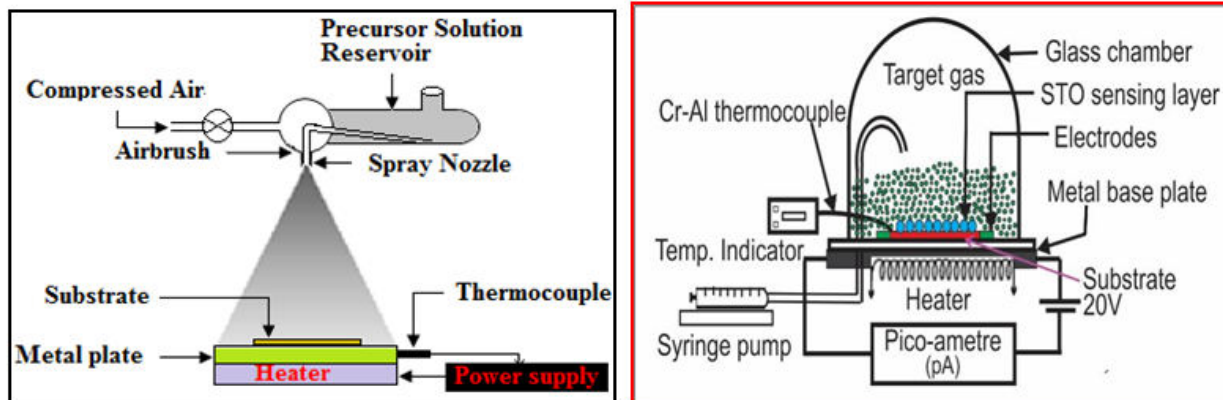


**Figure 1 (a).** Schematic diagram of thin film deposition by spray pyrolysis technique (b) Experimental setup used for gas response measurement.

## 2.2. Sensor performance

The performance of sensors was checked using a static system under laboratory conditions (Fig.1(b)). The samples were characterized for 30-3300 ppm concentration of CO various operating temperatures. The Gas response is defined as the ratio of change in conductance of the sample on exposure to a test gas to the conductance in the presence of air.

$$\text{Gas Response (S)} = \left| \frac{G_a - G_g}{G_a} \right| = \frac{\Delta G}{G_a}$$

Where-  $G_a$  is the conductance in air,  $G_g$  the conductance in a sample gas and  $\Delta G$  is the change in conductance.

The gas sensor system developed in the laboratory was employed for characterizing the sensor performance.

## 2.3. Fabrication of thin film resistor (TFR)

The thin film resistors were designed with a 2.5 cm × 1 cm area. The contacts were made by coating silver paste on thin film surface.

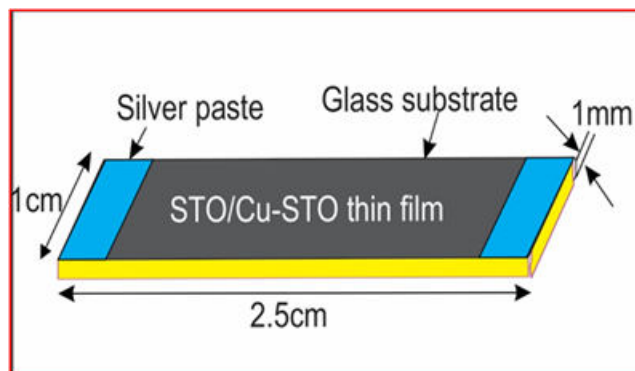


Figure 2. The schematic of the gas sensing device.

### 2.4. Structural Information of STO

In fig.3.the tetragonal structure of perovskites showing the local displacements leads to the variation in electric behaviour of this material. This compound, at above 120°C, exhibits a cubic structure while a lower symmetry, that is, a tetragonal unit cell at room temperature due to ions displacement. In this structure, the unit cell is not centrosymmetric and the crystal develops a permanent electric polarization as materials for gas sensors a result of ion displacements.

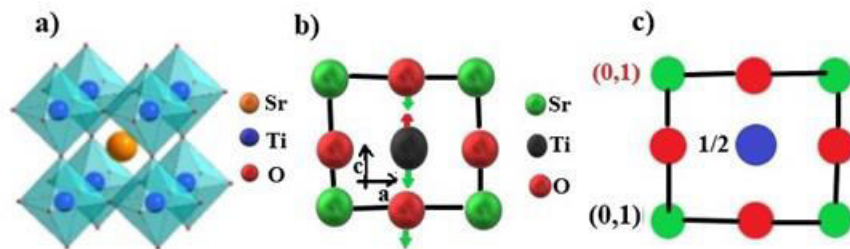


Figure 3. (a) octahedral sites (b) The local ion displacements of a tetragonal STO structure (c) its respective projection.

## 3.Result and Discussion

### 3.1 XRD of STO and Cu-STO thin films

In fig.4, depict the comparison XRD spectra of pure STO and Cu-doped STO with Cu 0.1wt% content. Diffraction maxima were observed in the diffraction spectra which are corresponding to the cubic perovskite lattice of STO.

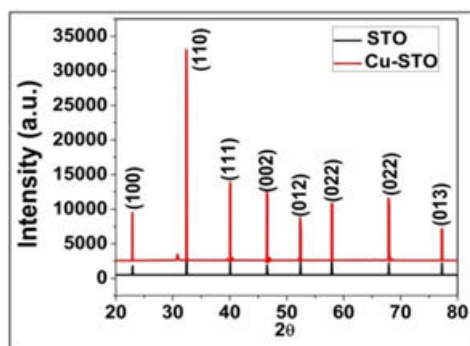


Figure.4. Figures show XRD profile of Cu<sub>1-x</sub>Sr<sub>x</sub>TiO<sub>3</sub> sample for Cu concentration of 0.1 weight percentage

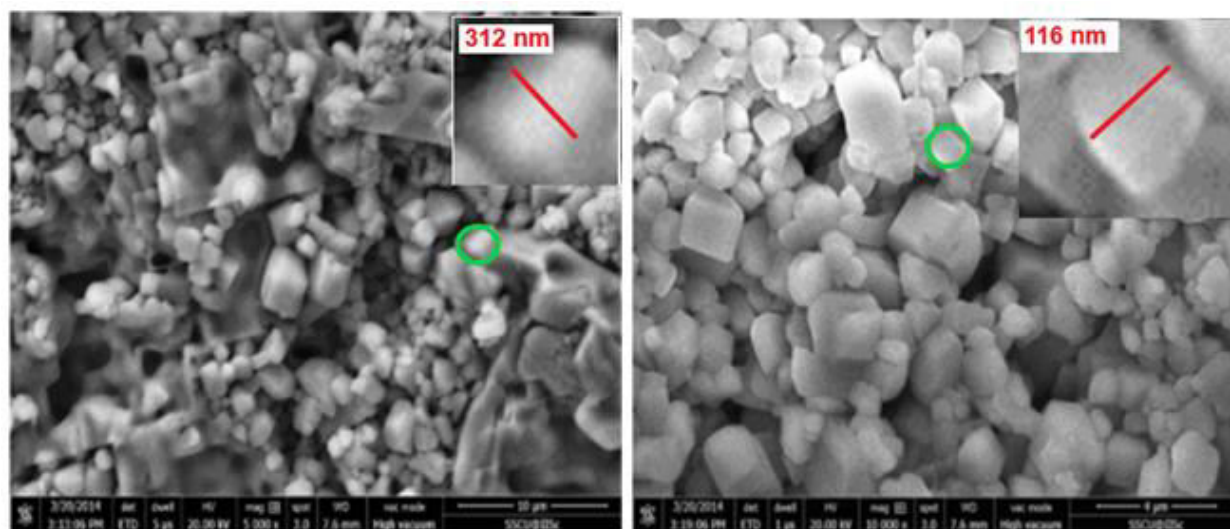
Table.1 Shows XRD profile data of CuO doped STO

| 2θ | d-spacing | FWHM | (hkl) | D (nm) | Px10 <sup>13</sup> | E <sub>strain</sub> |
|----|-----------|------|-------|--------|--------------------|---------------------|
|----|-----------|------|-------|--------|--------------------|---------------------|

| (Å <sup>0</sup> ) |        |        | (m <sup>-2</sup> ) |       |       |        |
|-------------------|--------|--------|--------------------|-------|-------|--------|
| 22.842            | 3.8930 | 0.0818 | (100)              | 110.1 | 8.25  | 0.0149 |
| 32.492            | 2.7550 | 0.0697 | (110)              | 131.8 | 5.76  | 0.0435 |
| 40.049            | 2.2506 | 0.0723 | (111)              | 129.8 | 5.94  | 0.0145 |
| 46.56             | 1.9498 | 0.0781 | (002)              | 123.1 | 6.59  | 0.0074 |
| 52.439            | 1.7441 | 0.1132 | (012)              | 86.9  | 13.24 | 0.0273 |
| 57.865            | 1.5928 | 0.0896 | (112)              | 112.6 | 7.89  | 0.0487 |
| 67.908            | 1.3795 | 0.0939 | (022)              | 113.3 | 7.79  | 0.0658 |
| 77.26             | 1.2342 | 0.1063 | (013)              | 106.3 | 8.85  | 0.0377 |

The decreasing value of lattice parameter (a) of copper doped STO was clearly observed in ref [24] at low concentrations. Similar reports were achieved in the present investigation. The lattice parameter of pure STO was reported in ref [25] and in the present case ‘a’ value was slightly decreased to 0.3893nm. Since the ionic radius of Cu<sup>+2</sup> (0.121nm) is smaller than that of Sr<sup>+2</sup> (0.144nm). Charge compensation can be obeyed if copper ion occupies the strontium site while it cannot be satisfied if Cu<sup>+2</sup> ions are substituted in Ti<sup>+4</sup> sites and oxygen vacancy can be created. However, this diminishes the lattice parameter. The structure factor (F) is responsible for the enormous enhancement of intensity of the diffraction lines in spectrum. The space group was identified as Pm3m. Furthermore the average crystalline size (D=114.9nm) using Scherer formula, average dislocation density ( $\rho=8.03 \times 10^{13} \text{m}^{-2}$ ) and average elastic strain ( $E_{\text{strain}}=0.0324$ ) were estimated using proper formulae. XRD data is represented in the table 1.

### 3.2. FE- SEM analysis



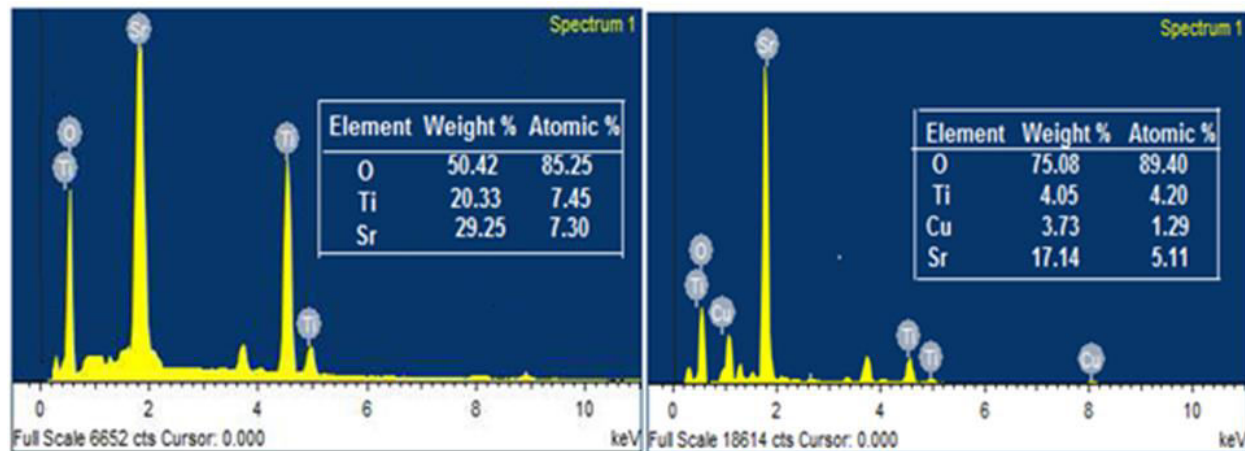


**Figure 5.** Micrographs of (a) STO (b) CuO-STO samples

From fig.5 it can be seen that the surface morphology was studied by FESEM with magnifications 5000x and 10000x over the range 10  $\mu\text{m}$  and 4  $\mu\text{m}$ . Obviously, uniformity in the distribution of grains and grain boundaries was observed. The dimensions are calculated by Image software. The grain size of STO and Cu-STO thin films are 312 nm and 116 nm respectively.

### 3.3. EDS Spectrum of STO and Cu-STO films

Stoichiometric mass % of Sr, Ti and O in  $\text{SrTiO}_3$  are 25.77, 60.12 and 14.11 respectively. Elemental analysis showed that, the mass % of Sr, Ti and O in  $\text{SrTiO}_3$  are not as per the Stoichiometric proportion.

**Figure 6.** EDS spectrum of (a)STO (b) Cu-STO samples

This is very advantageous for gas sensing applications as smaller grain size has a larger specific area and as a result, gas response increases. From the FE-SEM pictures, it can be concluded that the average grain size of sensing layer is less than 10 $\mu\text{m}$ . This is very advantageous for gas sensing applications as smaller grain size has a larger specific area and as a result, gas response increases.

## 4. Gas sensing properties

### 4.1. Sensing performance of pure and modified STO

The response of STO to CO increases with operating temperature, reaches maximum at 300 $^{\circ}\text{C}$  and decreases with further increase in operating temperature. Gas response was increased for modified STO. Response to CO gas is related generally to adsorption of oxygen ions on the surface of the film with a CO gas.

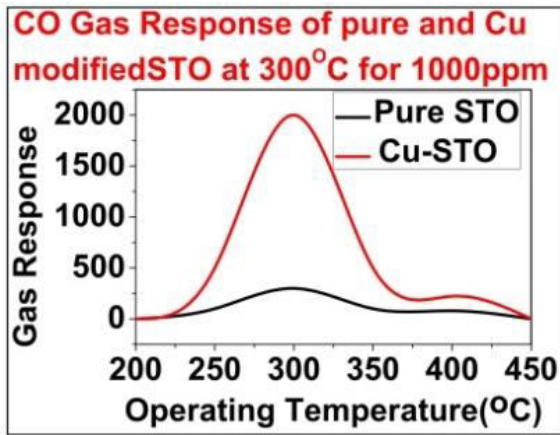


Figure 7 (a)

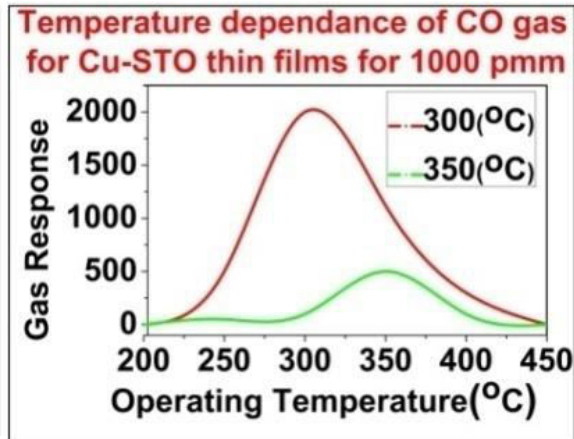


Figure 7(b)

Fig. 7. (a) Variation of gas response of thin films of pure and modified STO with operating temperature (b) Temperature dependence of gas response (c) Active region of sensor

#### 4.2. Variation of gas response to modified STO

Fig.8(a) depicts the variation of gas responses of pure STO and eight gases tested as a function of operating temperature. It is clear from the figure that pure STO based sensor showed highest gas response (300) at 300°C and 2000 at 300°C for Cu-STO.

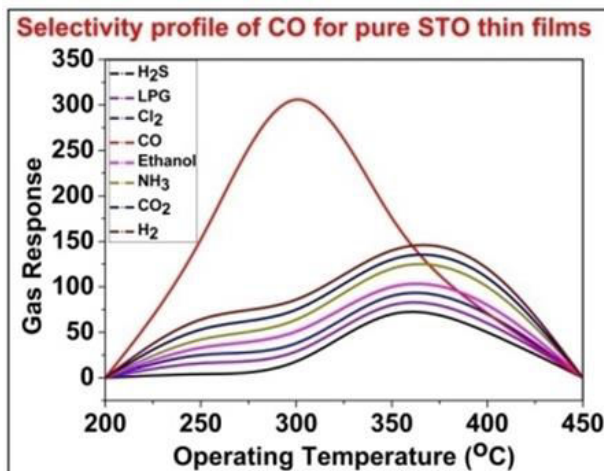


Figure 8 (a)

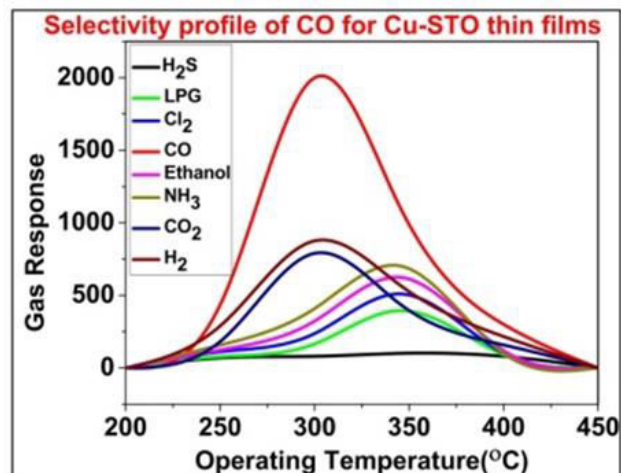


Figure 8 (b)

Figure 8. Temperature dependence of gas response (a) Variation of gas response of thin films of pure and (b modified STO with operating temperature

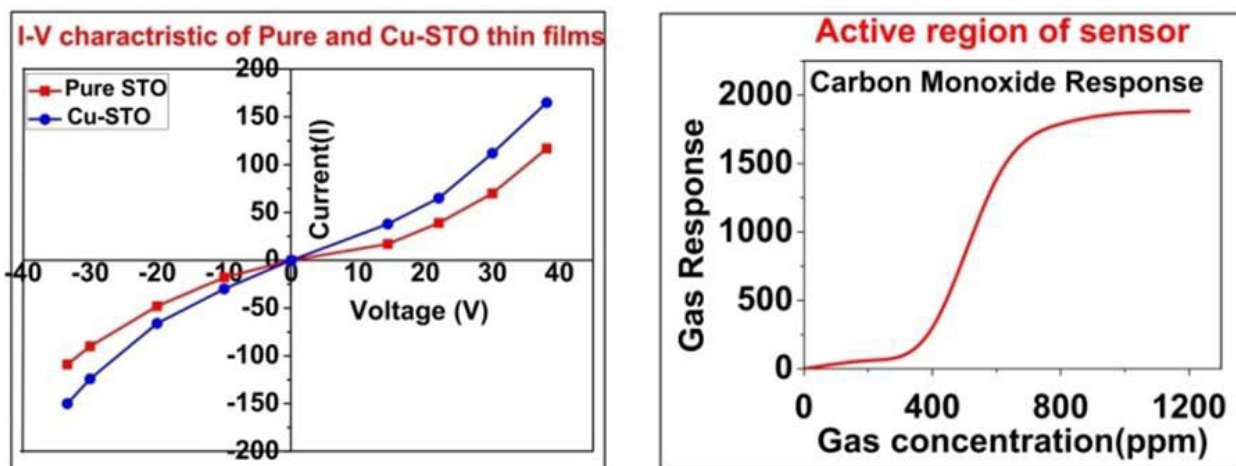


Figure 9 (a)

Figure 9 (b)

Figure 9. (a) Conductivity-temperature profile. (b) Active region of sensor

This sensor could therefore be used as temperature tuned sensor. At 300<sup>0</sup>C CO gas acquire a positive charge which, in case of n-type STO, causes release of further conduction electrons and shown sensitivity to CO gas. It is clear from figures that CuO-modified STO show maximum response to CO. Amongst all CuO-modified STO thin film showed highest gas response 2000 to CO. Fig.9 (b) shows variation of gas response of most sensitive CuO-modified STO film to CO as a function of gas concentration. The response values are observed to increase continuously with increasing gas concentration up to 800 ppm. The rate of increase of response is slower up to 400 ppm, then increases linearly up to 1000 ppm and finally it goes to saturation. Thus, the active region of the sensor would be up to 1000 ppm. At lower gas concentrations, the unimolecular layer of gas molecules would be formed on the surface of the sensor, which could interact more actively giving larger response. The multilayer of gas molecules, on the sensor surface, at the higher gas concentrations would result into saturation in response beyond 1000 ppm gas.

## 5. Electrical properties and Electrical Conductivity

The nature of I-V characteristics is approximately symmetrical which shows that the contacts are expected to be ohmic in nature. It is observed from Fig.9(c) that the resistance of pure STO film is smaller than that of modified films. The resistances of other films are larger, which could be attributed to segregation of CuO at intergrain boundaries. The CuO-modified STO film consists of large number of smaller particles of Cu-species distributed around the larger particles on the surface of the STO film. The CuO grains may reside in the intergranular region of STO, resulting in developing of intergrain boundaries and intergranular potential barriers. The conductivity values of samples in Fig.10 increase with operating temperature. The increase in conductivity with increasing temperature could be attributed to negative temperature coefficient of resistance and semiconducting nature of the CuO-activated STO films. The adsorption chemistry of CuO-modified STO surface differs from the pure STO thick film surface. The CuO misfits on the surface would adsorb more oxygen species than the pure STO surface. The conductivity of the



20min. film is more in comparison of other films this may attributed to CuO molecules are more in mass% onto surface of the film.

### 6. Carbon monoxide sensing mechanism

In figure 11 , At these temperatures, oxygen is adsorbed at the metal oxide surface by trapping electrons from the bulk material. The result is an overall decrease or increase in the metal oxide resistance, depending on whether the material is n-type or p-type, respectively.

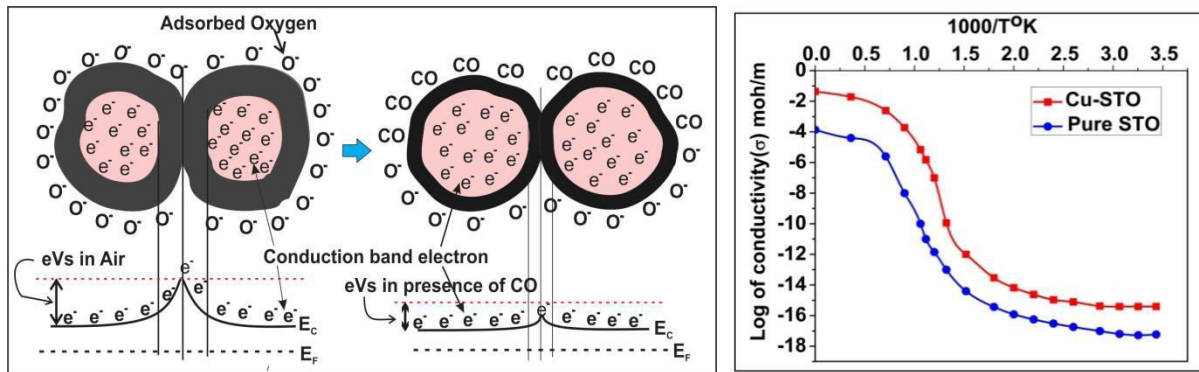


**Figure 10.** Gas sensing function and conduction mechanism for a porous Cu-STO, where the oxygen and carbon monoxide gas can penetrate to interact with each grain. **Fig.11.** Conductivity temperature profile.

The band bending at the metal oxide/ambient interface is depicted in Figure 10. The introduction of a target gas in the atmosphere causes a reaction with the oxygen, removing it from the interface and reducing the band bending effect and, thereby, the overall resistance. [26].

### 8. Warm-up, response/recovery time

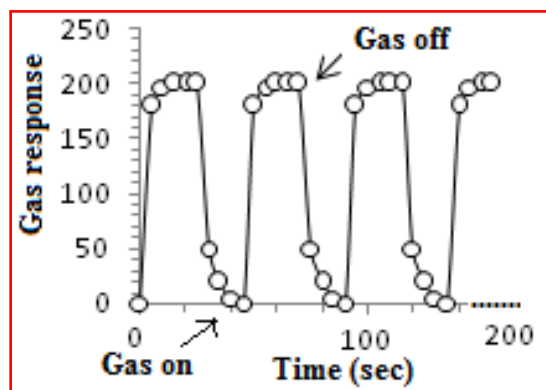


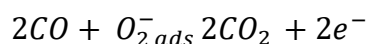
**Figure 12.** Warm up time, Response/recovery time of sensor.

The time required to reach the operating condition is called the warm-up time of a sensor material. The target gas is allowed to fall on the sensor element. The average sensitivity of 200, average response time of 25 seconds and average recovery time (corresponding to complete or 100% recovery) of 45 seconds are noted. The time for 80% recovery was however, less than 25 seconds

and beyond this time, the sensor can be considered to be ready for the next sensing cycle. The time required to reach the operating condition is called the warm-up time of a sensor material. The target gas is allowed to fall on the sensor element. The average sensitivity of 2000, average response time of 25 seconds and average recovery time (corresponding to complete or 100% recovery) of 45 seconds are noted. The time for 80% recovery was however, less than 25 seconds and beyond this time, the sensor can be considered to be ready for the next sensing cycle. The stabilization of the sensor response results from the equilibration of the chemisorption process. The most stable species at 300 °C is the  $O^-$  species and the stabilization was achieved when an equilibrium concentration of these adsorbed species was obtained.

## 9. Discussion

It is well known that the sensitivity of the metal-oxide semiconductor sensors is mainly resolute by the interactions between CO and the surface of the sensor. So, it is obvious that for the greater specific surface area of the materials, the interaction between the adsorbed gases and the sensor surface will be stronger, *i.e.* sensitivity will be higher. The gas sensing properties of materials are relative to the surface of the materials. The gases are always adsorbed and even react with the surface. So, small particle size and large specific area contribute to oxygen and CO adsorption on the surface of the materials, which is responsible for the increase in sensitivity of the sensor. Thus, during oxidation CO liberates electrons into the conduction band, thereby decreasing the resistance of the film upon exposure to CO. The change of electrical properties of the metal oxide semiconductor due to adsorption of gas molecules is responsible for STO and Cu-STO sensor response, which is due to surface interactions between the tin oxide and the surrounding gases. The oxygen from the air was adsorbed onto the surface of the Cu-STO thin film. Electrons from the surface region of the Cu-STO were transferred to the adsorbed oxygen, leading to the formation of an electron-depleted region near the surface of the Cu-STO film. The electron depleted region, where electron density is less, is an area of high resistance and the core region of the film, where electron densities are high, is an area of relatively low resistance. The form of the adsorbed oxygen becomes  $O^-$  and  $-2O$  species have been observed. When the thin film of STO and Cu-STO is exposed to a reducing gas like CO, surface reaction is took place



due to which electrons were released and the electrons released from surface reaction transfer back into the conduction band leading to a decrease in the resistance and an increase in the conductance of Cu-STO thin film.

## 10. Conclusion

From the results, following statements can be made for the sensing performance of the present CuO-modified sensors.

1. Using spray pyrolysis technique, the STO and Cu-STO thin films are successfully prepared.
2. The CO gas sensing properties of the pure and CuO modified STO were investigated.

3. The films exhibited cubic structure having single perovskite phases with the exception of few additional phases corresponding to the presence of TiO<sub>2</sub> rutiles and SrCu<sub>3</sub>Ti<sub>4</sub>O<sub>12</sub> phases.
4. The optimum operating temperature, for a CO concentration of 1000 ppm, was 300 °C.
5. The pure STO showed poor response to CO gas but response was enhanced for Cu-doped STO thin films by the virtue of doping of copper.
6. CuO was observed to be good promoter in gas sensing performance of STO based gas sensors.
7. The sensor has good selectivity for CO against Cl<sub>2</sub>, LPG, NH<sub>3</sub>, CO<sub>2</sub>, H<sub>2</sub>, H<sub>2</sub>S and Ethanol, gases at low temperature.
8. The response and recovery times were found to be 25 s and 45 s respectively. Such times are considered to be adequately fast for gas-sensing applications.
9. The sensor device can be fabricated for CO gas sensing from ambient environment.

## References

1. Dionigi M.; Ferroni,; Faglia G.;Sberveglieri. G. ; *Sensors and Actuators B*,**2008**,130, 567.
2. Lim H.M.; Lee D. Y.; Oh Y. J., *Sensors and Actuators A*, **2006**,125, 405.
3. Qian H. L.; Wang K.; Li Y.; Fang H. T.; Q. H. Lu; Q. H.; Max L.; *Mater. Chem. Phys.* **2006**,100, 82.
4. Ramirez F. F.; Tarancon F; Casals O.; Arbiol J.; Rodriguez A. R.; Morante J. R., *Sensors and Actuators B*, **2007**,121, 3.
5. . Kim I. J; Han S. D.; Gwak J.; Hong D. U.; Jakhar D.; Singh K. C.; Wang J. S, *Sensors and Actuators B*,**2007**, 127, 44.
6. C. Han, D. S. Han, and S. P. Khatkar, *Sensors*, **2006**,6, 492.
7. Muthaiah S.,Kien W. *Review on Sensing Applications of Perovskite Nanomaterials, Chemosensors*, **2020**, 8, 55.
8. Wagh M.S.; Patil L. A.; Tanay S.,; Amalnerker D. P.; *Mate. Chem. Phys*,**2004**, 84 228-233.
9. Shind V. K.; Gujar T. P.; Lokhande C. D.; Mane R. S.; Han S. H., *Sensors and Actuators B* , **2007**,123, 882.
10. Manjula P.S., Arunkumar, Sunkara V.M.. Au/SnO<sub>2</sub> an Exellent Material for Room Temperature Carbon Monoxide Sensing,**2010**.
11. Comini E.; Faglia G.; Sberveglieri G.; Pon Z.; Wang Z. L.; *Appl. Phys. Lett.* **2002** 81, 1869
12. Vaishnav V. S.; Patel P. D. ; Patel N. G., *Thin Solid Films*, **2005**,490, 94 .

13. Gorley P. M.; Khomyak V. V.; Bilichuk S. V.; Orletsky I. G.; Hovly P. P. ; Grechko V. O., *Mater. Sci. and Eng. B* ,**2005**,118, 160.
14. Mamazza Jr., Morel D. L; Ferekider C. S.; *Thin Solid Films* , **2005**,484, 26 .
15. Yoo K. S.; Park S. H.; Karg J. H., *Sensors and Actuators B* , **2005**,180, 159.
16. Yang H. T. ; Cheung Y. T.; *Jr. Crystal Growth*, **1982**,56, 429 .
17. Hui F., Miller T. M.; Magruder R. M.; Weller R. A., *J. Appl. Phys.*, **2002**,91, 6194.
18. Lane D. W.; Coath J. A., K. D. Rogers K. D.; Hunnikin B. J. ; Beldon H. S.' *Thin Solid Films* , **1992**, 221, 262.
19. Paraguay F;, Estrada D. W.; Acosta L. D. R.; Andra; MikiYoshidaM., *Thin Solid Films* , **1999**,350, 192 .
20. Blandenet G.; Court M. ; Lagarde Y.; *Thin Solid Films*, **1981**,77, 81 .
21. Culha O.; Ebeoglugil M. F.; Birlik I.; Celik E.; Toparli M., *J. Sol-Gel. Sci. Technol.* **2009**,51, 32.
22. Chatelon J. P.; Tenier C.; Bemstein E.; Berjoan R. ; Roger J. A., *Thin Solid Films* ,**1994**,247, 162.
23. Oreal B.; Lavrencic-Stangar U.; Cmjak O.; Bukovea P. ; Kosec M., *J. NonCryst. Solids*, **1994**,167, 272.
24. Alicia A.; Terry G.; Holesinger, P.; Clem,V.;Matias,; Jia Q.X.;Haiyan W.;Steve R.F.;Brady G.,*IEEE transactions on applied superconductivity*,. **2005**,15,.2.
25. Alastair George Hartley Smith, **2011**, PhD thesis.
26. Barsan, N.; Weimar, U. Fundamentals of Metal Oxide Gas Sensors. In Proceedings of the 14<sup>th</sup> International Meeting on Chemical Sensors, Nuremberg, Germany, **2012**,20–23 ,618–621.